Metagenome-genome-wide association studies reveal human genetic impact on the oral microbiome

Xiaomin Liu[1,2], Xin Tong[1], Jie Zhu[1], Liu Tian[1], Zhuye Jie[1,3], Yuanqiang Zou[1,3,4], Xiaoqian Lin[1,5], Hewei Liang[1], Wenxi Li[1,5], Yanmei Ju[1,2], Youwen Qin[1], Leying Zou[1], Haorong Lu[6], Xun Xu[1], Huanming Yang[1,7], Jian Wang[1,7], Yang Zong[1], Weibin Liu[1], Yong Hou[1], Shida Zhu[1], Xin Jin[1], Huijue Jia[1,8,†], Tao Zhang[1,3,†]

1. BGI-Shenzhen, Shenzhen 518083, China;
2. College of Life Sciences, University of Chinese Academy of Sciences, Beijing 100049, China;
3. Department of Biology, University of Copenhagen, Universitetsparken 13, DK-2100 Copenhagen, Denmark;
4. Qingdao-Europe Advanced Institute for Life Sciences, BGI-Shenzhen, Qingdao 266555, China
5. School of Bioscience and Biotechnology, South China University of Technology, Guangzhou 510006, China
6. China National Genebank, BGI-Shenzhen, Shenzhen 518120, China;
7. James D. Watson Institute of Genome Sciences, Hangzhou 310058, China;
8. Shenzhen Key Laboratory of Human Commensal Microorganisms and Health Research, BGI-Shenzhen, Shenzhen 518083, China;

† To whom correspondence should be addressed: T.Z., tao.zhang@genomics.cn and H.J., jiahuijue@genomics.cn

Abstract

The oral microbiota contains billions of microbial cells, which could contribute to diseases in a number of body sites. Challenged by eating, drinking and dental hygiene on a daily basis, the oral microbiota is regarded as highly dynamic. Here, we report significant human genomic associations with the oral metagenome from more than 1,915 individuals, for both the tongue dorsum and saliva. Five genetic loci, *APPL2*, *SLC2A9 and MGST1* associated with tongue dorsum, *LOC102723769-OR11H1-POTEH* and *MTRNR2L1-LOC105371703-MIR4522* associated with salivary microbial features, reached study-wide significance ($p < 3.16 \times 10^{-11}$). Further analyses confirmed 6 genome-wide significant loci shared between tongue dorsum and saliva. For example, the dental caries pathogen *Prevotella melaninogenica* associated with *MARK2-RCOR2*; the periodontitis bacteria *Treponema* associated with *CCL26-CCL24* and *Porphyromonas* associated with *CSMD1* at both niches. Human genetics account for at least 10% of oral microbiome differences between individuals. Machine learning models showed that polygenetic risk score dominated over oral microbiome in predicting predisposing risk of dental diseases such as dental calculus and gingival bleeding. These findings indicate that human genetic differences are one explanation for a stable or recurrent oral microbiome in each individual.

Introduction

A health individual swallows 1-1.5 liters of saliva every day[1], the microbes in which could colonize the gut of susceptible individuals[2-5]. Oral metagenomic shotgun sequencing data has been available from the Human Microbiome Project (HMP)[6] , for rheumatoid arthritis[7] and colorectal cancer[3]. Other diseases such as liver cirrhosis, atherosclerotic cardiovascular diseases, type 2 diabetes, and colorectal cancer studied by metagenome-wide association studies (MWAS) using gut microbiome data also indicated potential contribution from the oral microbiome in disease etiology[2,8-11].

Controversy over human genetic versus environmental determination of the fecal microbiome is being clarified by an increasing number of studies[12-17]. The strongest signal in cohorts of European ancestry is the association between *LCT1* and *Bifidobacterium*, explained by metabolism of lactose by the commensal bacterium. These large-scale genome-wide association studies have mainly focused on fecal microbiome, however, the influence of host genetics on the composition and stability of the oral microbiome is still poorly understood. Several studies based on 16S rRNA amplicon sequencing and microarrays have reported that human oral microbiota is influenced by both host genetics and environmental factors[18-21]. Only two studies have identified human genes that affected oral microbial communities. One study identified that *IMMPL2* on chromosome 7 and *INHBA-AS1* on

chromosome 12 could influence microbiome phenotypes[19]. The other study reported that gene copy number (CN) of the *AMY1* locus correlated with oral and gut microbiome composition and function[22]. These two studies used 16S rRNA amplicon sequencing for a small number of samples. Therefore, host genetics affecting the human oral microbiome and their impact on disease remain to be investigated.

Here, we presented the first large-scale metagenome-genome-wide association studies (M-GWAS) using high-depth sequencing data for both whole genome and oral metagenome, in a cohort of 2,984 healthy Chinese individuals, of which all individuals had whole genome data and over 1,915 individuals had matched tongue dorsum and salivary samples. A large number of concordant associations were identified between genetic loci and the tongue dorsum and salivary microbiomes. The effects of environmental factors and host genes on oral microbiome composition were investigated. Host genetics explained more variance of microbiome composition than environmental factors. The findings underscore the value of M-GWAS for *in situ* microbial samples, instead of focusing on feces.

Results

The oral microbiome according to metagenomically assembled microbial genomes

The 4D-SZ cohort (multi-omics, with more data to come, from Shenzhen, China) at present have high-depth whole-genome sequencing data from 2,984 individuals (mean depth of 33×, ranged from 21× to 87×, **Supplementary Table 1, Supplementary Fig. 1**). Among these, over 1,915 individuals had matched tongue dorsum and salivary samples for M-GWAS analysis.

Shotgun metagenome sequencing was performed for the 3,932 oral samples, with an average sequencing data of 20.07 ± 7.66 Gb for 2,017 tongue dorsum and 15.68 ± 3.21 Gb for 1,915 salivary samples (**Supplementary Table 1, Supplementary Fig. 1**). The microbiome composition was determined according to alignment to a total of 56,213 metagenome-assembled genomes (MAGs) that have been organized into 3,589 species-level clusters (SGBs) together with existing genomes, of which 40% (1,441/3,589) was specific in this cohort[23]. Both the tongue dorsum and the salivary samples contained the phyla *Bacteroidetes* (relative abundance of 37.2 ± 11.3% for tongue dorsum and 40.1 ± 10.2% for saliva, respectively), *Proteobacteria* (30.1 ± 16.5% and 30.6 ± 13.1%, respectively), *Firmicutes* (20.5 ± 8.2% and 17.7 ± 6.7%, respectively), *Actinobacteriota* (4.3 ± 3.4% and 2.6 ± 2.0%, respectively), *Fusobacteriota* (4.0 ± 1.9% and 3.3 ± 1.4%, respectively), *Patescibacteria* (in Candidate Phyla Radiation, CPR, 2.5 ± 1.6% and 3.1 ± 1.6%,

respectively) and *Campylobacterota* (1.1 ± 0.9% and 1.3 ± 0.8%, respectively) (**Supplementary Fig. 2a-b**).These seven phyla cover between 99.7% (tongue dorsum) and 98.7% (saliva) of the whole community, indicating that the two oral sites share a common core microbiota. Consistent with HMP results using 16S rRNA gene amplicon sequencing[24], the salivary samples presented a higher alpha diversity than tongue dorsum samples (mean Shannon index of 6.476 vs 6.228; Wilcoxon Rank-Sum test $p < 2.2 \times 10^{-16}$; **Supplementary Fig. 2c**). The microbiome compositions calculated by beta-diversity based on genus-level Bray–Curtis dissimilarity slightly differed (explained variance $R^2 = 0.055$, $p < 0.001$ in permutational multivariate analysis of variance (PERMANOVA) test; **Supplementary Fig. 2d**).

Host genetic variants strongly associated with the tongue dorsum microbiome

With this so-far the largest cohort of whole genome and whole metagenome data, we first performed M-GWAS on the tongue dorsum microbiome. With the 1,583 independent tongue dorsum microbial taxa ($r^2 < 0.8$ from 3177 taxa total), and 10 million human genetic variants (minor allele frequency (MAF) ≥ 0.5%), 1,677 associations involving 345 independent loci ($r^2 < 0.2$) reached genome-wide significance ($p < 5 \times 10^{-8}$). With a more conservative *Bonferroni*-corrected study-wide significant *p* value of 3.16×10^{-11} (= 5×10^{-8} / 1,583), we identified 3 genomic loci, namely *APPL2*, *SLC2A9 and MGST1,* associated with 5 tongue dorsum microbial features involving 112 SNP-taxon associations (**Fig. 1a**). These associations showed remarkable evidence of polygenicity and pleiotropy (**Fig. 1b**). There was no evidence of excess false positive rate in the GWAS analysis (genomic inflation factors λ_{GC} ranged from 0.981 to 1.023 with median 1.005; **Supplementary Fig. 3a**). All genome-wide significant associations were listed in **Supplementary Table 2**.

The strongest association was on rs1196764 located in the *APPL2* locus, correlated with dozens of microbial taxa, with positive associations with three species, namely *Prevotella jejuni* ($p = 6.89 \times 10^{-14}$), unclassified SGB (uSGB) 3339 belonging to the genus *Oribacterium* ($p = 9.99 \times 10^{-12}$) and uSGB 315 belonging to the genus *Solobacterium* (an anaerobic gram-positive bacterium associated with colorectal cancer[25]; $p = 2.12 \times 10^{-11}$). *APPL2* encoded a multifunctional adapter protein that binds to various membrane receptors, nuclear factors and signaling proteins to regulate many processes, such as cell proliferation, immune response, endosomal trafficking and cell metabolism.

The second strongest association was on rs3775944 ($p = 5.09 \times 10^{-13}$), which is a perfect proxy for the exonic variant rs10939650 ($r^2 = 0.99$) in *SLC2A9.* Minor alleles of these variants negatively correlated with *Oribacterium* uSGB 1215*. SLC2A9* is a

urate transporter and *SLC2A9* polymorphisms have been reported associated with serum uric acid and urine uric acid concentration in multiple studies[26-28]. We also looked at these top loci in Biobank Japan[29,30], and *SLC2A9* was correlated with lower serum uric acid concentration (**Supplementary Fig. 4;** $p = 5.56 \times 10^{-184}$), ischemic stroke ($p = 1.73 \times 10^{-4}$), urolithiasis ($p = 2.02 \times 10^{-4}$) and pulse pressure ($p = 6.86 \times 10^{-4}$). The negative associations with serum uric acid concentration ($p = 6.74 \times 10^{-6}$) and urine pH ($p = 8.75 \times 10^{-4}$) were confirmed in this cohort. Notably, *SLC2A9 locus* not only negatively correlated with serum uric acid, but also negatively correlated with its associated bacteria *Oribacterium* uSGB 1215 that was observed increasing risk of serum uric acid ($\beta = 0.08$; $p = 3.15 \times 10^{-5}$). Similarly, *LPL* was associated with abundance of *Haemophilus D parainfluenzae A* ($p = 1.59 \times 10^{-8}$) and triglyceride concentration (**Supplementary Fig. 4;** $p = 5.93 \times 10^{-56}$), and consistently *Haemophilus D parainfluenzae A* correlated with triglyceride concentration ($p = 7.70 \times 10^{-16}$). These findings suggested that host genes, microbiomes and gene-microbiome interactions might codetermine host phenotype.

Variants in *MGST1* were identified as the third strongest signal, with minor alleles negatively associated with *Streptococcus* uSGB 2460 ($p = 1.50 \times 10^{-11}$), followed by family Streptococcaceae and other eight Streptococcus SGBs, such as *S. infantis* and *S. pseudopneumoniae*. These variants were also positively associated with red blood cell count ($p = 2.51 \times 10^{-5}$) and asthma ($p = 5.03 \times 10^{-5}$) in Biobank Japan. Consistently, 84% (237/282) of the *Streptococcus spp.* were observed correlated with red blood cell count ($p < 0.05$), such as *S. mitis* ($p = 1.99 \times 10^{-12}$) and *S. pseudopneumoniae* ($p = 4.51 \times 10^{-12}$). These results suggested that commensal *Streptococcus* species might utilize red blood cells as camouflage to avoid being engulfed by phagocytic immune cells in addition to the well-known group A Streptococcus (*S. pyogenes*)[31]. Our results also supported previous findings that *Streptococcus spp.* are often involved in diseases of the respiratory tracts such as asthma[32].

M-GWAS of the salivary microbiome confirm and extend human genetic contribution to the oral microbiome

The saliva may appear more dynamic than the tongue dorsum, and the microbiome composition involves multiple niche in the oral cavity[33]. We next tried M-GWAS analysis for the saliva microbiome. With the 1,685 independent salivary microbial taxa ($r^2 < 0.8$ from 3,677 taxa total), and 10 million human genetic variants (MAF ≥ 0.5%), 2,455 associations involving 374 independent loci ($r^2 < 0.2$) reached genome-wide significance ($p < 5 \times 10^{-8}$). Similar to tongue dorsum M-GWAS analyses, the genomic inflation factors of these salivary M-GWAS tests showed no inflation (λ_{GC} ranged from 0.978 to 1.022 with median 1.002; **Supplementary Fig. 3b**). All genome-wide significant associations were listed in **Supplementary Table 3**. With a more conservative *Bonferroni*-corrected study-wide significant p-value of

2.97× 10^{-11} (= 5 × 10^{-8} / 1,685), we identified 2 study-wise significant independent loci (**Fig. 2a**). One genetic locus, spanning three genes *LOC102723769*, *OR11H1* and *POTEH*, associated with species *F0422 uSGB 392* belonging to family Veillonellaceae (leading SNP rs4911713; p = 2.11 × 10^{-12}). The other locus, *MTRNR2L1-LOC105371703-MIR4522*, associated with genus *Eggerthia* (leading SNP rs36186689; p = 8.85 × 10^{-12}). This locus regulated the expression of *FLJ36000* in both brain cerebellar hemisphere (p = 6.74× 10^{-6}) and testis (p = 8.58× 10^{-12}). The two loci were most associated with serum testosterone level and work stress, respectively, while searching GWAS summary statistics from Biobank Japan and this study. In addition, we found four loci associated with both salivary microbiome and metabolic traits or diseases at genome-wide significance: *DPEP2/NFATC3* that associated with species *Lancefieldella sp000564995* was linked to high density lipoprotein cholesterol (HDLC); *PDXDC2P-NPIPB14P* associated with species *Centipeda sp000468035* linked to thyroid abnormality; *LARP1* associated with species *Aggregatibacter kilianii* linked to mean corpuscular hemoglobin; *SMARCA1* associated with species *Veillonella parvula* linked to pharyngeal mucosal congestion (PMC) (**Supplementary Fig. 5**).

Among 345 and 374 independent loci associated with tongue dorsum and salivary microbiome (p < 5 × 10^{-8}), respectively, 6 loci were shared between them (**Fig. 2b**): *MARK2-RCOR2* associated with *Prevotella* (most associated species *P. melaninogenica* for tongue dorsum and *P. uSGB 1369* for saliva), *APPL2* associated with *Oribacterium uSGB 3339*, *LOC105374972-NRSN1* associated with *Lancefieldella uSGB 2019*; *CCL26-CCL24* associated with *Treponema uSGB 706*; and *CSMD1* associated with *Porphyromonas* (most associated species *P. uSGB 2049* for tongue dorsum and *P. uSGB 414* for saliva). *RTTN-SOCS6* associated with Firmicutes *uSGB 1705*. 339 loci were genome-wide significant for the tongue dorsum samples, and also showed p-values between 0.01 and 5 × 10^{-8} for the salivary samples. For example, *SLC2A9*, a determinant of low uric acid (UA) concentration, showed the strongest association with SGBs belonging to *Oribacterium* (p = 5.09 × 10^{-13}) and *Lachnoanaerobaculum* (p = 4.69 × 10^{-9}) in tongue dorsum samples, and also relative low association with that of *Oribacterium* (p = 0.001) and *Lachnoanaerobaculum* (p = 1.0 × 10^{-4}) in salivary samples. Similarly, *SHB-ALDH1B1* and SGBs of genus *Streptococcus*, *PAG1-FABP5* and *Pseudomonas E marginalis*, *GJB6-CRYL1* and *Capnocytophaga sp002209445*, *AQP7P1-LINC00537* and *uSGB 297* belonging to genus *Catonella*, all exhibited stronger associations in tongue dorsum samples (p < 5 × 10^{-9}) than in saliva (p > 0.001). Likewise, 368 loci were genome-wide significant for the saliva, and also showed p-values between 0.05 and 5 × 10^{-8} for the tongue dorsum, although the top two study-wide significant loci for saliva didn't reach suggestive significance in tongue dorsum samples (p > 1 × 10^{-5}). Our M-GWAS of the salivary microbiome further confirm and extend human genetic contribution to the oral microbiome. These results suggested tongue and salivary microbiome as niches in one oral cavity shared high level of host genetic similarity in co-evolution process.

Gene set enrichment analysis for oral M-GWAS signals

To explore the potential functions of the identified M-GWAS signals for tongue dorsum and salivary, we annotated the genetic associations and performed functional mapping and gene sets enrichment analysis with the DAVID[34] and FUMA[35] platform (Methods), followed by disease enrichment and tissue expression analysis. M-GWAS analysis returned 221 and 261 genes (<20kb for associated genetic loci) for tongue dorsum and salivary microbiome, respectively. Functional mapping of their separately related genes in DAVID database suggested that tongue dorsum associated host genes mainly enriched in phosphatidylinositol-related pathways including phosphatidylinositol signaling system, biosynthesis, dephosphorylation and phosphatidylinositol-3,4,5-trisphosphate 5-phosphatase activity, and Ca^{2+} pathway including calcium ion binding, calcium channel regulator activity and voltage-gated calcium channel activity (**Supplementary Table 4**). Phosphatidylinositol signaling system have been reported to be higher in the gut microbiota of centenarians[36] and consistently decreased in saliva microbiota of RA patients[37]. Saliva associated host genes mainly enriched in cardiomyopathy including arrhythmogenic right ventricular-, hypertrophic- and dilated cardiomyopathy, glycerophospholipid metabolism and choline metabolism in cancer (**Supplementary Table 5**).

The GAD_Disease (Genetic Association Disease Database) segment analysis in DAVID showed that both tongue dorsum and saliva M-GWAS signals were enriched in cardiometabolic diseases and traits such as tobacco use disorder, myocardial infarction, triglycerides, blood pressure, lipoproteins, coronary artery disease, and nervous system diseases such as schizophrenia, bipolar disorder, psychiatric disorders and Parkinson's disease (**Tables S4 and S5**). Positional mapping in GWAS catalog using FUMA tool showed the similar diseases enriched results with that of using GAD catalog in DAVID. Genotype-Tissue Expression (GTEx) analysis on saliva microbiome associated host genes exhibited an enrichment for genes expressed in brain (anterior cingulate cortex BA24 and substantia nigra) and cells of EBV-transformed lymphocytes (**Supplementary Fig. 6**).

Host genetics influence oral microbiome more than environment

We first investigate the contribution of environmental factors to oral microbiome β-diversity (based on genus-level Bray–Curtis dissimilarities), by using host metadata including age, gender, BMI, dietary, lifestyle, drug use and health status questions, as well as blood measurements. We selected 340 independent variables out of the

total 423 environmental factors for association analysis (correlation $r^2 < 0.6$). A total of 35 and 53 factors were significantly associated with β-diversity (BH-adjusted FDR < 0.05) for tongue dorsum and salivary samples, respectively, via PERMANOVA analysis (**Supplementary Fig. 8; Supplementary Tables 6 and 7**). Of these, high sugar and high fat food frequency and dental calculus were the strongest associated factors for both tongue dorsum and salivary microbial compositions. A high sugar diet increased the abundances of some specific bacteria such as *Streptococcus mutans* that metabolized sugar to acids and caused dental caries. In this cohort, high sugar and high fat food frequency significantly increased the abundances of *Gemella haemolysans* (β = 0.21; p =2.92 × 10^{-19}) and *Streptococcus parasanguinis* (β = 0.18; p = 7.56 × 10^{-16}) in salivary samples. In total, 35 and 53 factors were able to infer 6.36% and 7.78% of the variance of microbiome β-diversity for tongue dorsum and salivary samples, respectively. When calculating the cumulative explained variance of β-diversity by using all the independent environmental variables, we found that 12.85% and 15.54% of the variance can be explained for tongue dorsum and salivary samples, respectively.

We next evaluated the effect of host genetics on oral microbiome compositions. We performed association analysis for *α*-diversity and *β*-diversity using 10 million genetic variants (MAF ≥ 0.5%). Six genome-wide significant loci were identified for *α*-diversity for oral microbiome (**Supplementary Table 8**). Four loci, *NFIB*, *LINC02578*, *LOC105373105* and *EIF3E*, associated with *α*-diversity of tongue dorsum samples. Two loci, *SLC25A42* and *LINC02225*, associated with *α*-diversity of salivary samples. In the association analysis between genetic variation and microbiome β-diversity, we found one locus for tongue dorsum samples and one locus for salivary samples with marginal genome-wide significance ($p < 5 \times 10^{-8}$; **Supplementary Fig. 9**), respectively. One SNP, rs545425011 located in *DNAJC12* was associated with microbial composition of tongue dorsum ($p = 1.07 \times 10^{-8}$). When searching its correlations with microbial taxa, it was mostly negatively associated with *Leptotrichia A sp000469505* and *Prevotella saccharolytica* (**Supplementary Table 9**), however, positively associated with *Rothia* SGBs such as *R. mucilaginosa which* was dominant in tongue dorsum and often observed in large patches toward the exterior of the consortium. The other SNP, rs73243848 located in *G2E3-AS1* was associated with salivary microbial composition ($p = 2.35 \times 10^{-8}$). It was mostly positively associated with *Prevotella* uSGB 2511 and family Bacteroidaceae (**Supplementary Table 10**).

The above analysis found that 53 and 35 factors (BH P <0.05) explained 7.78% and 6.36% of the β-diversity variance for salivary and tongue dorsum microbiome, respectively. By applying the same number of SNPs that were most closely associated with β-diversity, we identified 14.14% and 10.14% of the β-diversity variance could be inferred for salivary and tongue dorsum microbiome, respectively (**Supplementary Fig. 10**). The findings suggested host genetics is likely to influence oral microbiome more than environment.

Host genetics and oral microbiome predict dental diseases

The dynamic and polymicrobial oral microbiome is a direct precursor of diseases such as dental calculus and gingival bleeding. To understand the aggregate effect of host genetic variants and oral microbiome on dental diseases, we constructed models using genetic polygenic risk scores (PRS) and oral microbiome separately, as well as their combination, to predict dental diseases. We found 2 of the 6 dental diseases occurred in over 5% individuals to be significantly associated with the oral microbiome (**Fig. 3a**; FDR $p< 0.001$). Either of salivary and tongue dorsum microbiome explained 20% of the variance for dental calculus. Salivary and tongue dorsum microbiome explained 13% and 15% of the variance for gingival bleeding, respectively. Compared with oral microbiome, the genetic PRS showed significantly higher predictive efficiency with a mean R^2 of 45%, ranging from the lowest of 25% for gingival bleeding to highest of 60% for teeth loss. Furthermore, when incorporating the oral microbiome into PRS model, the predictive efficiency is slightly improved, with a 4% increasement of R^2 for dental calculus and a 6% increasement of R^2 for gingival bleeding (**Fig. 3b**).

The discriminative efficiency for dental diseases was also evaluated using area under the curve (AUC; **Fig. 3c**). Salivary and tongue dorsum microbiome had a good discrimination for dental calculus (AUC=0.81 and 0.80, respectively), and a median discrimination for gingival bleeding (AUC=0.72 and 0.73, respectively). The models of PRS had AUC of 0.93-0.94 for 5 of the 6 dental diseases, except for gingival bleeding (AUC=0.78). Incorporating the oral microbiome into PRS model resulted in improved discrimination with AUC increasing from 0.94 to 0.97 for dental calculus and from 0.78 to 0.83 for gingival bleeding. These results may help explain why some people are genetically predisposed to the major dental diseases.

Discussion

In summary, we performed the first large-scale M-GWAS for oral microbiome and report unequivocal human genetic determinants for the oral microbiome. Our M-GWAS analysis identified a big amount of concordant association signals shared by tongue dorsum and salivary microbiome, with all genome-wide significant associations in one niche (**Fig. 2b**; $p < 5 \times 10^{-8}$) were also at least nominally significant in the other niche ($p < 0.01$), consistent with our and previous findings that tongue dorsum and salivary microbiome communities exhibited high levels of similarity[38,39], especially in micron-scale structure of oral niches[33,40]. Consistent with previous studies[24,41], the salivary microbiome showed higher alpha diversity than tongue dorsum. In combination with the fact that saliva comes into contact with all surfaces in the oral cavity and represents a fingerprint of the general composition of the oral microbiome, these results suggested that salivary microbiome is more

diverse and likely more dynamic. Thus, host genetic associations that are stronger with the salivary than the tongue dorsum community will further invite other omics studies, especially the proteome and the nitrogen cycle that could impact microbial growth.

Host-associated microbial communities are influenced by both host genetics and environmental factors. The debate centers on the relative contributions of host genetic and environmental factors to human microbiome. Twins modeling have demonstrated that some taxa of the human oral microbiome are heritable[18,19], however, some studies indicated oral microbiome variances were shaped primarily by the environment rather than host genetics[20,21]. With this high-depth whole genome and metagenomic sequencing and high-quality assembled oral microbiome samples, we found that significant environmental factors explained 6.36%-7.78% of the β-diversity variance for oral microbiome, however, the same number of significant SNPs could infer 10.14%-14.14% of the β-diversity variance for oral microbiome (**Supplementary Fig. 7 and 9**). These findings indicated host genetics is likely to influence oral microbiome more than environment.

As the genetics are already there at birth, oral hygiene would be more important for people who are more likely to develop dental diseases and beyond. Despite different aetiologias, dental calculus and gingival bleeding are both driven by a combined function of the oral microbiota and host factors. However, dental caries, teeth defect and loss were mainly determined by host genetics and less influenced by oral microbiome in this cohort. These results help us to better understand the pathogenic mechanisms and aided the design of personalized therapeutic approaches for different oral diseases. These results also provide a rational for repeatedly taking oral samples, to study the mostly stable human genome, long-term trends and short-term dynamics in the oral microbiome.

Methods

Study subjects

All the adult Chinese individuals in this cohort were recruited for a multi-omics study, with some volunteers having samples from as early as 2015, which would constitute the time dimension in '4D'. The cohort included 2,984 individuals with blood samples collected during a physical examination in 2017 in the city of Shenzhen and all these individuals were enlisted for high-depth whole genome sequencing (**Supplementary Table 1**). 3,932 (2,017 tongue dorsum and 1,915 saliva) oral samples from this cohort were newly collected for whole metagenomic sequencing

between 2017 to 2018 (**Supplementary Table 1**). The protocols for blood and oral collection, as well as the whole genome and metagenomic sequencing were similar to our previous literature[5,23,42]. For blood sample, DNA was extracted using MagPure Buffy Coat DNA Midi KF Kit (no. D3537-02) according to the manufacturer's protocol. Tongue dorsum and salivary samples were collected with MGIEasy kit. For salivary sample, a 2x concentration of stabilizing reagent kit was used and 2 mL saliva was collected. DNA of oral samples was extracted using MagPure Stool DNA KF Kit B (no. MD5115-02B). The DNA concentrations from blood and oral samples were estimated by Qubit (Invitrogen). 500 ng of input DNA from blood and oral samples were used for library preparation and then processed for paired-end 100bp sequencing using BGISEQ-500 platform[43].

The study was approved by the Institutional Review Boards (IRB) at BGI-Shenzhen, and all participants provided written informed consent at enrolment.

High-depth whole genome sequence for this cohort

2,984 individuals with blood samples were sequenced to a mean of 33x for whole genome. The reads were aligned to the latest reference human genome GRCh38/hg38 with BWA[44] (version 0.7.15) with default parameters. The reads consisting of base quality <5 or containing adaptor sequences were filtered out. The alignments were indexed in the BAM format using Samtools[45] (version 0.1.18) and PCR duplicates were marked for downstream filtering using Picardtools (version 1.62). The Genome Analysis Toolkit's (GATK[46], version 3.8) BaseRecalibrator created recalibration tables to screen known SNPs and INDELs in the BAM files from dbSNP (version 150). GATKlite (v2.2.15) was used for subsequent base quality recalibration and removal of read pairs with improperly aligned segments as determined by Stampy. GATK's HaplotypeCaller were used for variant discovery. GVCFs containing SNVs and INDELs from GATK HaplotypeCaller were combined (CombineGVCFs), genotyped (GenotypeGVCFs), variant score recalibrated (VariantRecalibrator) and filtered (ApplyRecalibration). During the GATK VariantRecalibrator process, we took our variants as inputs and used four standard SNP sets to train the model: (1) HapMap3.3 SNPs; (2) dbSNP build 150 SNPs; (3) 1000 Genomes Project SNPs from Omni 2.5 chip; and (4) 1000G phase1 high confidence SNPs. The sensitivity threshold of 99.9% to SNPs and 98% to INDELs were applied for variant selection after optimizing for Transition to Transversion (TiTv) ratios using the GATK ApplyRecalibration command.

We applied a conservative inclusion threshold for variants: (i) mean depth >8×; (ii) Hardy-Weinberg equilibrium (HWE) $P > 10^{-5}$; and (iii) genotype calling rate > 98%. We demanded samples to meet these criteria: (i) mean sequencing depth > 20×; (ii) variant calling rate > 98%; (iii) no population stratification by performing principal components analysis (PCA) analysis implemented in PLINK[47] (version 1.9) and (iv) excluding related individuals by calculating pairwise identity by descent (IBD, Pi-hat threshold of 0.1875) in PLINK. No samples were removed in quality control filtering. After variant and sample quality control, 2,984 individuals with about 10 million common and low-frequency (MAF ≥ 0.5%) variants were left for subsequent

analyses.

Oral metagenomic sequencing and quality control

Metagenomic sequencing was done on the BGISEQ-500 platform, with 100bp of paired-end reads for all samples and four libraries were constructed for each lane. We generated 15.68 ± 3.21Gb (average ± standard deviation) raw bases per sample for salivary samples and 20.07 ± 7.66 raw bases per sample for tongue dorsum samples (**Supplementary Table 1**). After using the quality control module of metapi pipeline followed by reads filtering and trimming with strict filtration standards(not less than mean quality phred score 20 and not shorter than 51bp read length) using fastp v0.19.463, host sequences contamination removing using Bowtie2 v2.3.564 (hg38 index) and seqtk65 v1.3, we finally got an average of 3.1Gb (host rate:77%) and 9.9Gb (host rate:31%) raw bases per sample for salivary and tongue dorsum samples, respectively.

Oral metagenomic profiling

The high-quality oral genome catalogue was constructed in our previous study[23]. The oral metagenomic sequencing reads was mapped to oral genome catalogue (http://ftp.cngb.org/pub/SciRAID/Microbiome/human_oral_genomes/bowtie2_index) using Bowtie2 with parameters : "--end-to-end --very-sensitive --seed 0 --time -k 2 --no-unal --no-discordant -X 1200", and the normalized contigs depths were obtained by using jgi_summarize_bam_contig_depths, then based on the correspondence of contigs and genome, the normalized contig depth were converted to the relative abundance of each species for each samples. Finally, we merged all representative species relative abundance to generate a taxonomic profile for human oral population. The profiling workflow was implemented in metapi jgi_profiling module (https://github.com/ohmeta/metapi/blob/dev/metapi/rules/profiling.smk#L305).

Tongue dorsum and salivary microbiome comparison

The nonparametric Wilcoxon rank-sum test was used to determine statistically significant differences in species α-diversity between tongue dorsum and saliva niches. We analyze the β-diversity (based on genus-level Bray–Curtis dissimilarity) difference between the two oral niches using PERMANOVA (adonis) in the 'vegan' package and visualize the two oral niches groups using ordination such as non-metric multidimensional scaling (NMDS) plots.

Association analysis for oral microbial taxa

After investigating the distributions of occurrence rate and relative abundance of all microbial taxa, we decided to filter the microbial taxa to keep those with occurrence rate over 90% and average relative abundance over 1×10^{-5}. After filtering, the represented genera of these microbial taxa covered between 99.63% (tongue dorsum) and 99.76% (saliva) of the whole community in the cohort. As many oral microbial taxa are highly correlated and aims to reducing the numbers of GWAS tests, we then performed a number of Spearman's correlation tests to obtain the independent taxa for M-GWAS analyses. Spearman's correlations were calculated

pairwise between all taxa, and the correlations used to generate an adjacency matrix where correlations of >0.8 represented an edge between taxa. A graphical representation of this matrix was then used for greedy selection of representative taxa. Nodes (microbiota taxa) were sorted by degree and the one with highest degree was then chosen as a final taxon (selecting at random in the case of a tie). The taxon and its connected nodes were then removed from the network and the process repeated until a final set of taxa sets were found such that each of the discarded taxon was correlated with at least one taxon. These filtering resulted in a final set of 1,583 and 1,685 independent microbial taxa for tongue dorsum and saliva, respectively, that were used for association analyses.

We tested the associations between host genetics and oral bacteria using linear model based on the relative abundance of oral bacteria. Specifically, the relative abundance was transformed by the natural logarithm and the outlier individual who was located away from the mean by more than four standard deviations was removed, so that the abundance of bacteria could be treated as a quantitative trait. Next, for 10 million common and low-frequency variants (MAF≥ 0.5%) identified in this cohort, we used a linear regression model to perform M-GWAS analysis via PLINK v1.9. Given the effects of environmental factors such as diet and lifestyles on microbial features, we included all potential cofounders that were significantly associated with the β-diversity (Benjamini–Hochberg FDR < 0.05) estimates in the below explained variance analysis, as well as the top four principal components (PCs) as covariates for M-GWAS analysis in both the salivary and tongue dorsum niches.

To investigate the correlations between the identified oral microbiome-related SNPs and diseases, we downloaded the summary statistics data from the Japan Biobank[29,30], a study of 300,000 Japanese citizens suffering from cancers, diabetes, rheumatoid arthritis and other common diseases. We searched the oral microbiome-related SNPs in the summary statistics data from Japan Biobank to examine their associations with diseases.

Functional and pathway enrichment analysis

The significant genetic variants identified in the association analysis were mapped to genes using ANNOVAR[48]. Given that some significant genetic variants were low-frequency in the M-GWAS results, it's most suitable to input gene lists for enrichment analysis. We mapped variants to genes based on physical distance within a 20kb window and got the gene lists for enrichment analysis. DAVID (https://david.ncifcrf.gov/) was utilized to perform functional and pathway enrichment analysis. DAVID is a systematic and integrative functional annotation tool for the analysis of the relevant biological annotation of gene lists and provide functional interpretation of the GO enrichment and KEGG pathway analysis[34]. The *p*-value <0.05 was considered statistically significant. In addition, the mapped genes were further investigated using the GENE2FUNC procedure in FUMA[35] (http://fuma.ctglab.nl/), which provides hypergeometric tests for the list of enriched mapping genes in 53 GTEx tissue-specific gene expression sets, 7,246 MSigDB

gene sets, and 2,195 GWAS catalog gene sets[35]. Using the GENE2FUNC procedure, we examined whether the mapped genes were enriched in specific diseases or traits in the GWAS catalog as well as whether showed tissue-specific expression. Significant results were selected if a false discovery rate (FDR)-corrected $p < 0.05$ was observed.

Association analysis for microbiome α-diversity and β-diversity

The microbiome β-diversity (between-sample diversity) based on genus-level abundance data were generated using the 'vegdist' function (Bray–Curtis dissimilarities). Then, we performed principal coordinates analysis (PCoA) based on the calculated beta-diversity dissimilarities using the 'capscale' function in 'vegan'. Finally, associations for β-diversity (a two-axis MDS) were performed using the manova() function from the 'stats' package, in a multivariate analysis using genotypes and the same covariates stated above as variables.

Association analysis for environmental factors

As part of the 4D-SZ cohort, all participants in this study had records of multi-omics data, including anthropometric measurement, stool form, defecation frequency, diet, lifestyle, blood parameters, hormone, etc.[21]. A total of 423 environmental factors are available in this cohort. Environmental metadata were first log-transformed and checked for collinearity using the Spearman correlation coefficient. Collinearity was assumed if a Spearman's $\rho > 0.6$ or $\rho < -0.6$. Collinear variables were considered redundant and one variable from each pair was removed from further analysis, resulting in a final set of 340 variables.

To investigate the potential associations of top loci identified in microbiome GWAS with environmental variables especially for serum metabolites, we also performed GWAS analysis for the 340 environmental variables. Among the 340 environmental traits, the log10-transformed of the mean-normalized values was calculated for each quantitative phenotype (such as amino acids, vitamins, microelements etc.) and a linear regression model for quantitative trait implemented in PLINK v1.9 was used for association analysis. Samples with missing values and values beyond 4 s.d. from the mean were excluded from association analysis. For each binary phenotype (such as diet, lifestyle etc.), a logistic regression model was used for association analysis. Age, gender and the top four PCs were included as covariates for each association analysis.

Environmental factors explained variance of oral microbiome

We next searched for associations between the 340 environmental variables selected above and the oral microbiome compositions. We performed Bray-Curtis distance-based redundancy analysis (dbRDA) to identify variables that are significantly associated with β-diversity and measure the fraction of variance explained by the factors, using the 'capscale' function in the vegan package. The significance of each response variable was confirmed with an analysis of variance (ANOVA) for the dbRDA (anova.cca() function in the vegan package). Only the

variables that were significantly associated (Benjamini–Hochberg FDR < 0.05) with the β-diversity estimates in the univariable models were included in the multivariable model. The additive explanatory value (in %) of significant response variables (e.g. environmental parameters, vitamins and serum amino acids etc.) was assessed with a variation partitioning analysis of the vegan package ('adj.r.squared' value using RsquareAdj option).

Construct PRS for diseases prediction

To obtain the predictions of human genetics on dental diseases, we used gradient boosting decision trees from the LightGBM (v.3.1.1) package[49] implemented in Python (v3.7.8) and fivefold cross validation scheme to construct risk-prediction models. In every fold of the fivefold cross validation scheme, we calculated the associations between SNPs and dental diseases within the training dataset, and then selected independent and significant SNPs (LD $r^2 < 0.2$, $p < 10^{-5}$) to calculate the PRS as an unweighted sum of risk alleles, and finally we trained a model on the PRS and predicted the disease risk in test dataset. During the process, we obtained the optimal values of the tuning parameters using fivefold cross validation and evaluated the results using the coefficient of determination (R^2) as variance explained and AUC as disease discriminative efficiency.

Data availability

All summary statistics that support the findings of this study including the associations between host genetics and tongue dorsum microbiome, host genetics and saliva microbiome are publicly available from https://db.cngb.org/search/project/CNP0001664. The release of these summary statistics data was approved by the Ministry of Science and Technology of China (Project ID: **, data has been uploaded and we are waiting for the approval ID of MOST). According to the Human Genetic Resources Administration of China regulation and the institutional review board of BGI-Shenzhen related to protecting individual privacy, sequencing data are controlled-access and are available via application on request (https://db.cngb.org/search/project/CNP0001664).

Acknowledgments

We sincerely thank the support provided by China National GeneBank. We thank all the volunteers for their time and for self-collecting the oral samples using our kit.

Author contributions

H.J. and T.Z. conceived and organized this study. J.W. initiated the overall health project. X.X., H.Y., S.Z., Y.H., Y.Zong and W.Liu contributed to organization of the cohort the sample collection and questionnaire collection. H.Lu led the DNA extraction and sequencing. X.Q., J.Z., R.W. generated the metabolic data. X.Liu, T.Z., and X.T. processed the whole genome data. Y.Zou, X.Lin, H.Liang, W.Li, Y.J., Y.Q. and L.Z. processed the metagenome data. X.Liu performed the metagenome-

genome-wide association analyses. X.Liu and H.J. wrote the manuscript. All authors contributed to data and texts in this manuscript.

Declaration of interests

The authors declare no competing financial interest.

Reference

1 Humphrey, S. P. & Williamson, R. T. A review of saliva: normal composition, flow, and function. *J Prosthet Dent* **85**, 162-169, doi:10.1067/mpr.2001.113778 (2001).

2 Atarashi, K. *et al.* Ectopic colonization of oral bacteria in the intestine drives TH1 cell induction and inflammation. *Science* **358**, 359-365, doi:10.1126/science.aan4526 (2017).

3 Schmidt, T. S. *et al.* Extensive transmission of microbes along the gastrointestinal tract. *Elife* **8**, doi:10.7554/eLife.42693 (2019).

4 Liu, X. *et al.* M-GWAS for the gut microbiome in Chinese adults illuminates on complex diseases. *bioRxiv* (2019).

5 Liu, X. *et al.* A genome-wide association study for gut metagenome in Chinese adults illuminates complex diseases. *Cell Discov* **7**, 9, doi:10.1038/s41421-020-00239-w (2021).

6 Human Microbiome Project, C. A framework for human microbiome research. *Nature* **486**, 215-221, doi:10.1038/nature11209 (2012).

7 Zhang, X. *et al.* The oral and gut microbiomes are perturbed in rheumatoid arthritis and partly normalized after treatment. *Nat Med* **21**, 895-905, doi:10.1038/nm.3914 (2015).

8 Qin, N. *et al.* Alterations of the human gut microbiome in liver cirrhosis. *Nature* **513**,

59-64, doi:10.1038/nature13568 (2014).

9 Jie, Z. *et al.* The gut microbiome in atherosclerotic cardiovascular disease. *Nature communications* **8**, 845, doi:10.1038/s41467-017-00900-1 (2017).

10 Qin, J. *et al.* A metagenome-wide association study of gut microbiota in type 2 diabetes. *Nature* **490**, 55-60, doi:10.1038/nature11450 (2012).

11 Yu, J. *et al.* Metagenomic analysis of faecal microbiome as a tool towards targeted non-invasive biomarkers for colorectal cancer. *Gut* **66**, 70-78, doi:10.1136/gutjnl-2015-309800 (2017).

12 Blekhman, R. *et al.* Host genetic variation impacts microbiome composition across human body sites. *Genome biology* **16**, 191, doi:10.1186/s13059-015-0759-1 (2015).

13 Bonder, M. J. *et al.* The effect of host genetics on the gut microbiome. *Nature genetics* **48**, 1407-1412, doi:10.1038/ng.3663 (2016).

14 Goodrich, J. K. *et al.* Genetic Determinants of the Gut Microbiome in UK Twins. *Cell host & microbe* **19**, 731-743, doi:10.1016/j.chom.2016.04.017 (2016).

15 Turpin, W. *et al.* Association of host genome with intestinal microbial composition in a large healthy cohort. *Nature genetics* **48**, 1413-1417, doi:10.1038/ng.3693 (2016).

16 Wang, J. *et al.* Genome-wide association analysis identifies variation in vitamin D receptor and other host factors influencing the gut microbiota. *Nature genetics* **48**, 1396-1406, doi:10.1038/ng.3695 (2016).

17 Rothschild, D. *et al.* Environment dominates over host genetics in shaping human gut microbiota. *Nature* **555**, 210-215, doi:10.1038/nature25973 (2018).

18 Gomez, A. *et al.* Host Genetic Control of the Oral Microbiome in Health and Disease.

Cell host & microbe **22**, 269-278 e263, doi:10.1016/j.chom.2017.08.013 (2017).

19 Demmitt, B. A. *et al.* Genetic influences on the human oral microbiome. *BMC genomics* **18**, 659, doi:10.1186/s12864-017-4008-8 (2017).

20 Freire, M. *et al.* Longitudinal Study of Oral Microbiome Variation in Twins. *Sci Rep* **10**, 7954, doi:10.1038/s41598-020-64747-1 (2020).

21 Shaw, L. *et al.* The Human Salivary Microbiome Is Shaped by Shared Environment Rather than Genetics: Evidence from a Large Family of Closely Related Individuals. *mBio* **8**, doi:10.1128/mBio.01237-17 (2017).

22 Poole, A. C. *et al.* Human Salivary Amylase Gene Copy Number Impacts Oral and Gut Microbiomes. *Cell host & microbe* **25**, 553-564 e557, doi:10.1016/j.chom.2019.03.001 (2019).

23 Zhu, J. *et al.* Over 50000 metagenomically assembled draft genomes for the human oral microbiome reveal new taxa. *bioRxiv* (2019).

24 Friedman, J. & Alm, E. J. Inferring correlation networks from genomic survey data. *PLoS Comput Biol* **8**, e1002687, doi:10.1371/journal.pcbi.1002687 (2012).

25 Jobin, C. Human Intestinal Microbiota and Colorectal Cancer: Moving Beyond Associative Studies. *Gastroenterology* **153**, 1475-1478, doi:10.1053/j.gastro.2017.10.030 (2017).

26 Lukkunaprasit, T. *et al.* The association between genetic polymorphisms in ABCG2 and SLC2A9 and urate: an updated systematic review and meta-analysis. *BMC Med Genet* **21**, 210, doi:10.1186/s12881-020-01147-2 (2020).

27 Ruiz, A., Gautschi, I., Schild, L. & Bonny, O. Human Mutations in SLC2A9 (Glut9)

667 Affect Transport Capacity for Urate. *Front Physiol* **9**, 476,
668 doi:10.3389/fphys.2018.00476 (2018).
669 28 Doring, A. *et al.* SLC2A9 influences uric acid concentrations with pronounced sex-
670 specific effects. *Nature genetics* **40**, 430-436, doi:10.1038/ng.107 (2008).
671 29 Ishigaki, K. *et al.* Large-scale genome-wide association study in a Japanese
672 population identifies novel susceptibility loci across different diseases. *Nature*
673 *genetics* **52**, 669-679, doi:10.1038/s41588-020-0640-3 (2020).
674 30 Kanai, M. *et al.* Genetic analysis of quantitative traits in the Japanese population
675 links cell types to complex human diseases. *Nature genetics* **50**, 390-400,
676 doi:10.1038/s41588-018-0047-6 (2018).
677 31 Wierzbicki, I. H. *et al.* Group A Streptococcal S Protein Utilizes Red Blood Cells as
678 Immune Camouflage and Is a Critical Determinant for Immune Evasion. *Cell Rep* **29**,
679 2979-2989 e2915, doi:10.1016/j.celrep.2019.11.001 (2019).
680 32 Teo, S. M. *et al.* The infant nasopharyngeal microbiome impacts severity of lower
681 respiratory infection and risk of asthma development. *Cell host & microbe* **17**, 704-
682 715, doi:10.1016/j.chom.2015.03.008 (2015).
683 33 Mark Welch, J. L., Ramirez-Puebla, S. T. & Borisy, G. G. Oral Microbiome
684 Geography: Micron-Scale Habitat and Niche. *Cell host & microbe* **28**, 160-168,
685 doi:10.1016/j.chom.2020.07.009 (2020).
686 34 Jiao, X. *et al.* DAVID-WS: a stateful web service to facilitate gene/protein list
687 analysis. *Bioinformatics* **28**, 1805-1806, doi:10.1093/bioinformatics/bts251 (2012).
688 35 Watanabe, K., Taskesen, E., van Bochoven, A. & Posthuma, D. Functional mapping

and annotation of genetic associations with FUMA. *Nature communications* **8**, 1826, doi:10.1038/s41467-017-01261-5 (2017).

36 Kim, B. S. *et al.* Comparison of the Gut Microbiota of Centenarians in Longevity Villages of South Korea with Those of Other Age Groups. *J Microbiol Biotechnol* **29**, 429-440, doi:10.4014/jmb.1811.11023 (2019).

37 Tong, Y. *et al.* Oral Microbiota Perturbations Are Linked to High Risk for Rheumatoid Arthritis. *Front Cell Infect Microbiol* **9**, 475, doi:10.3389/fcimb.2019.00475 (2019).

38 Rabe, A. *et al.* Metaproteomics analysis of microbial diversity of human saliva and tongue dorsum in young healthy individuals. *J Oral Microbiol* **11**, 1654786, doi:10.1080/20002297.2019.1654786 (2019).

39 Hall, M. W. *et al.* Inter-personal diversity and temporal dynamics of dental, tongue, and salivary microbiota in the healthy oral cavity. *NPJ Biofilms Microbiomes* **3**, 2, doi:10.1038/s41522-016-0011-0 (2017).

40 Wilbert, S. A., Mark Welch, J. L. & Borisy, G. G. Spatial Ecology of the Human Tongue Dorsum Microbiome. *Cell Rep* **30**, 4003-4015 e4003, doi:10.1016/j.celrep.2020.02.097 (2020).

41 Caselli, E. *et al.* Defining the oral microbiome by whole-genome sequencing and resistome analysis: the complexity of the healthy picture. *BMC Microbiol* **20**, 120, doi:10.1186/s12866-020-01801-y (2020).

42 Liu, X. *et al.* Inter-determination of blood metabolite levels and gut microbiome supported by Mendelian randomization. *bioRxiv* (2020).

43 Fang, C. *et al.* Assessment of the cPAS-based BGISEQ-500 platform for

711 metagenomic sequencing. *GigaScience* **7**, 1-8, doi:10.1093/gigascience/gix133
712 (2018).
713 44 Li, H. & Durbin, R. Fast and accurate short read alignment with Burrows-Wheeler
714 transform. *Bioinformatics* **25**, 1754-1760, doi:10.1093/bioinformatics/btp324 (2009).
715 45 Li, H. *et al.* The Sequence Alignment/Map format and SAMtools. *Bioinformatics* **25**,
716 2078-2079, doi:10.1093/bioinformatics/btp352 (2009).
717 46 McKenna, A. *et al.* The Genome Analysis Toolkit: a MapReduce framework for
718 analyzing next-generation DNA sequencing data. *Genome Res* **20**, 1297-1303,
719 doi:10.1101/gr.107524.110 (2010).
720 47 Purcell, S. *et al.* PLINK: a tool set for whole-genome association and population-
721 based linkage analyses. *Am J Hum Genet* **81**, 559-575, doi:10.1086/519795 (2007).
722 48 Wang, K., Li, M. & Hakonarson, H. ANNOVAR: functional annotation of genetic
723 variants from high-throughput sequencing data. *Nucleic Acids Res* **38**, e164,
724 doi:10.1093/nar/gkq603 (2010).
725 49 Ke, G. *et al.* LightGBM: A Highly Efficient Gradient Boosting Decision Tree. *NIPS*
726 *conference* (2017).
727
728

Figure captions

Fig. 1. Host genetic signals associated with tongue dorsum microbiome. (**a**). Manhattan plot shows the genetic variants associated with the tongue dorsum microbial taxa. The horizontal grey and black lines represent the genome-wide ($p = 5 \times 10^{-8}$) and study-wide ($p = 3.16 \times 10^{-11}$ for 1,583 independent M-GWAS tests) significance levels, respectively. Three loci that associated with tongue dorsum microbiome and reached study-wide significance were marked in red. Their located genes and associated microbial taxa with *p* values of < 3.16×10^{-11} were also listed. (**b**). Network representation of the 345 gene-microbiome associations identified in the tongue dorsum M-GWAS at the genome-wide significance. Each node represents either a gene (blue diamonds) or a microbial taxon (circles with different colors according to phylum). Each edge is an association between one gene and one microbial taxon. The bold edge represented study-wide significant associations as showed in (**a**). The genes that linked to at least two different microbial taxa from different phyla were also listed.

Fig. 2. Host genetic signals associated with salivary microbiome. (**a**). Manhattan plot shows the genetic variants associated with the salivary microbial taxa. The horizontal grey and black lines represent the genome-wide ($p = 5 \times 10^{-8}$) and study-wide ($p = 2.97 \times 10^{-11}$ for 1,685 independent M-GWAS tests) significance levels, respectively. Two loci that associated with salivary microbiome and reached study-wide significance were marked in red. Their located genes and associated microbial taxa with *p* values of < 2.97×10^{-11} were also listed. (**b**). *p*-values comparisons of the 345 and 374 independent loci associated with tongue dorsum and salivary microbiome ($p < 5 \times 10^{-8}$), respectively. The 6 genome-wide significant loci shared by tongue dorsum and salivary microbiome were listed.

Fig. 3. Oral microbiome and genetic PRS infer a significant fraction of the variance of dental diseases. (**a**) R^2 estimates of six dental diseases and their significance contributed by oral microbiome, evaluated using linear model in lightGBM package. * $p < 0.05$, ** $p < 0.01$ and *** $p < 0.001$. (**b**) Predictive efficiency of six dental diseases (measured using coefficient of determination (R2)), evaluated using a linear model under five different sets of predictive features: (i) relative abundances of salivary microbial taxa; (ii) relative abundances of tongue dorsum microbial taxa; (iii) PRS calculated as an unweighted sum of risk alleles from independent and significant SNPs (LD $r^2 < 0.2$, $p < 10^{-5}$) for each oral disease; (iv) 'PRS + salivary microbiome': PRS, relative abundances of salivary microbial taxa and (v) 'PRS + tongue microbiome': PRS, relative abundances of tongue dorsum microbial taxa. (**c**) The discriminative efficiency for six dental diseases (measured using area under the curve (AUC)), evaluated using a discriminative model under five different sets of predictive features as described in (**b**).

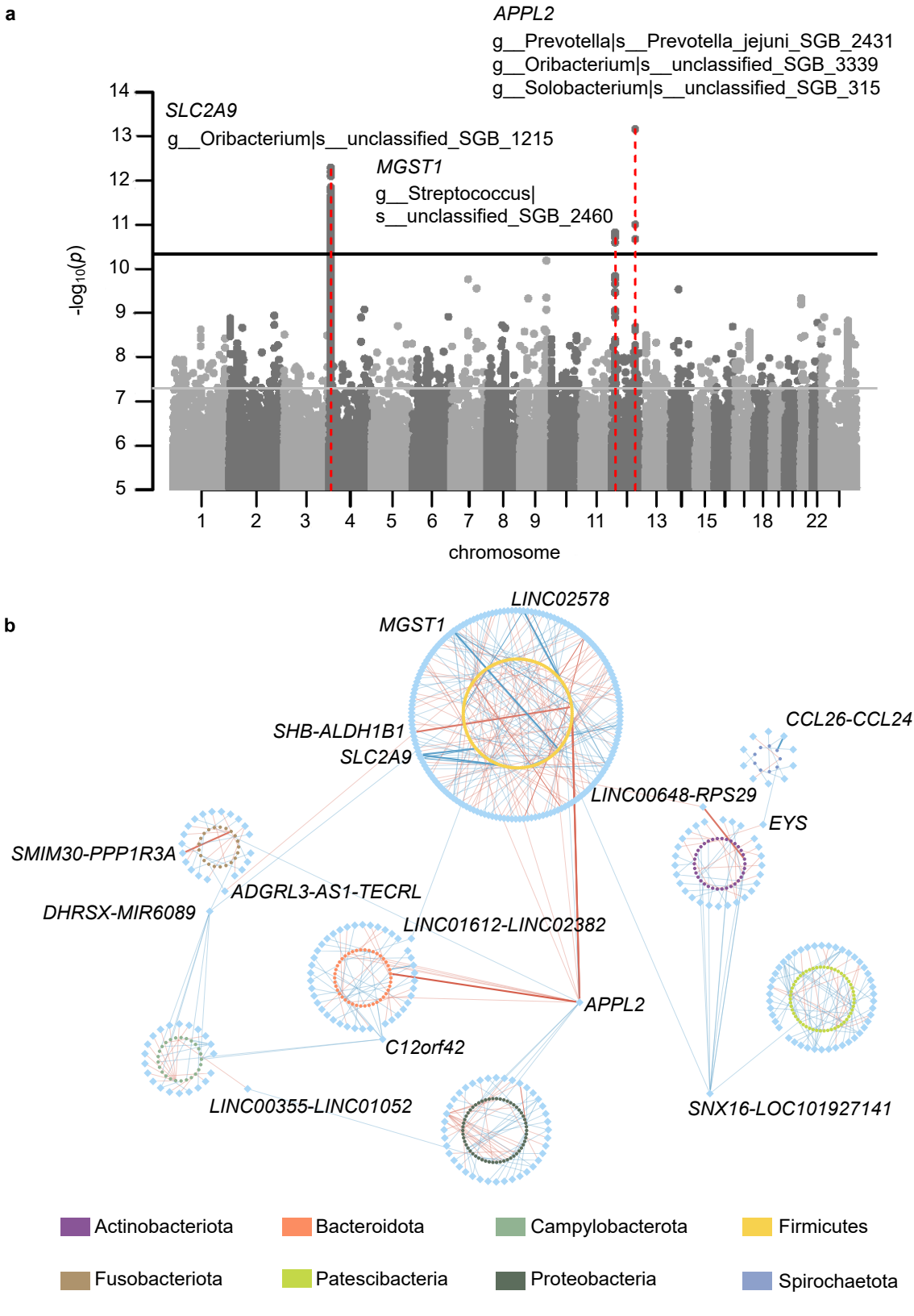
a
APPL2
g__Prevotella|s__Prevotella_jejuni_SGB_2431
g__Oribacterium|s__unclassified_SGB_3339
g__Solobacterium|s__unclassified_SGB_315
SLC2A9
g__Oribacterium|s__unclassified_SGB_1215
MGST1
g__Streptococcus|
s__unclassified_SGB_2460
-log10(p)
chromosome
b
LINC02578
MGST1
SHB-ALDH1B1
SLC2A9
CCL26-CCL24
LINC00648-RPS29
EYS
SMIM30-PPP1R3A
ADGRL3-AS1-TECRL
DHRSX-MIR6089
LINC01612-LINC02382
APPL2
C12orf42
LINC00355-LINC01052
SNX16-LOC101927141
Actinobacteriota
Bacteroidota
Campylobacterota
Firmicutes
Fusobacteriota
Patescibacteria
Proteobacteria
Spirochaetota

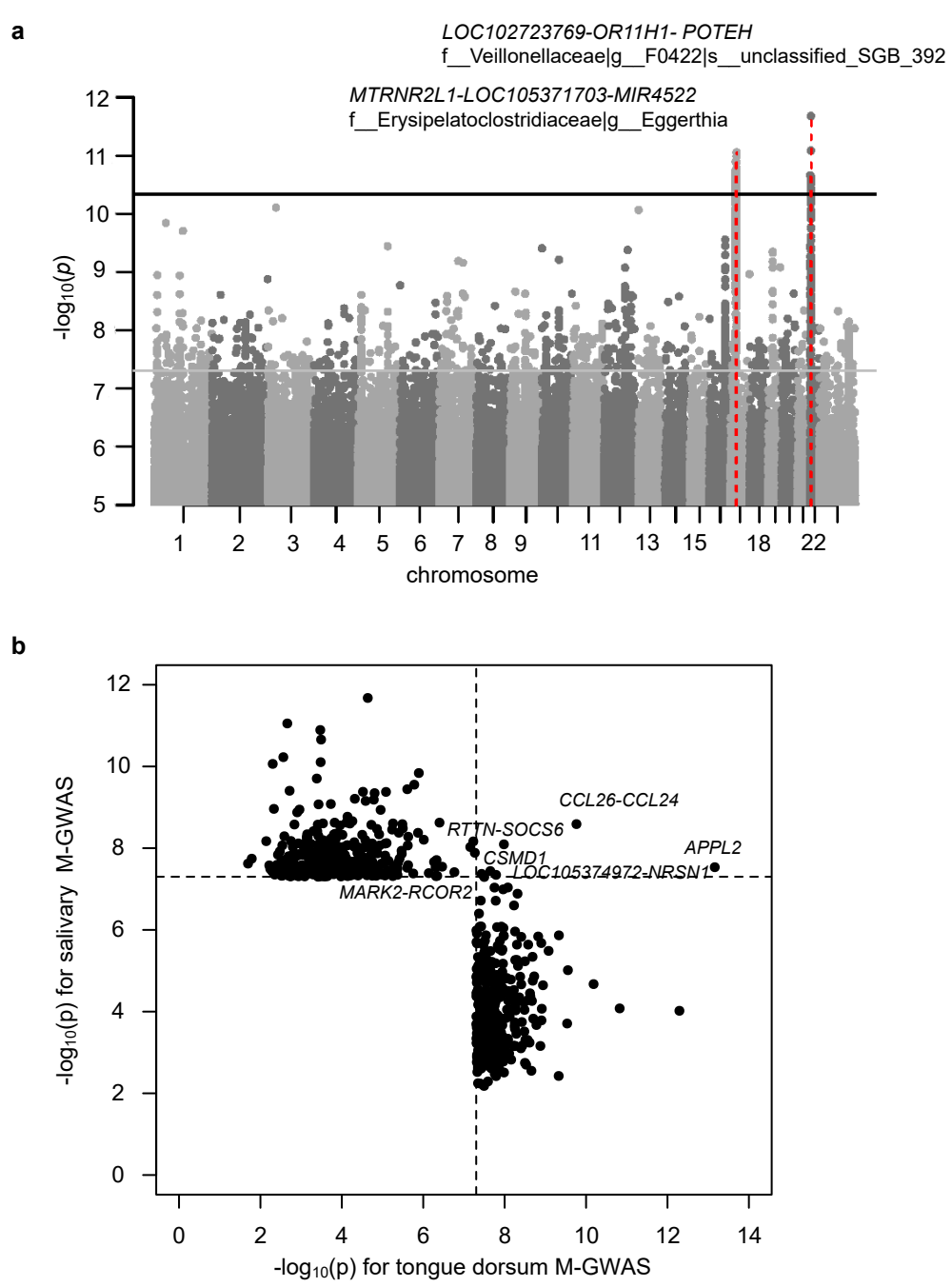
a
LOC102723769-OR11H1- POTEH
f__Veillonellaceae|g__F0422|s__unclassified_SGB_392
MTRNR2L1-LOC105371703-MIR4522
f__Erysipelatoclostridiaceae|g__Eggerthia
-log10(p)
chromosome
b
-log10(p) for salivary M-GWAS
-log10(p) for tongue dorsum M-GWAS
CCL26-CCL24
RTTN-SOCS6
APPL2
CSMD1
LOC105374972-NRSN1
MARK2-RCOR2

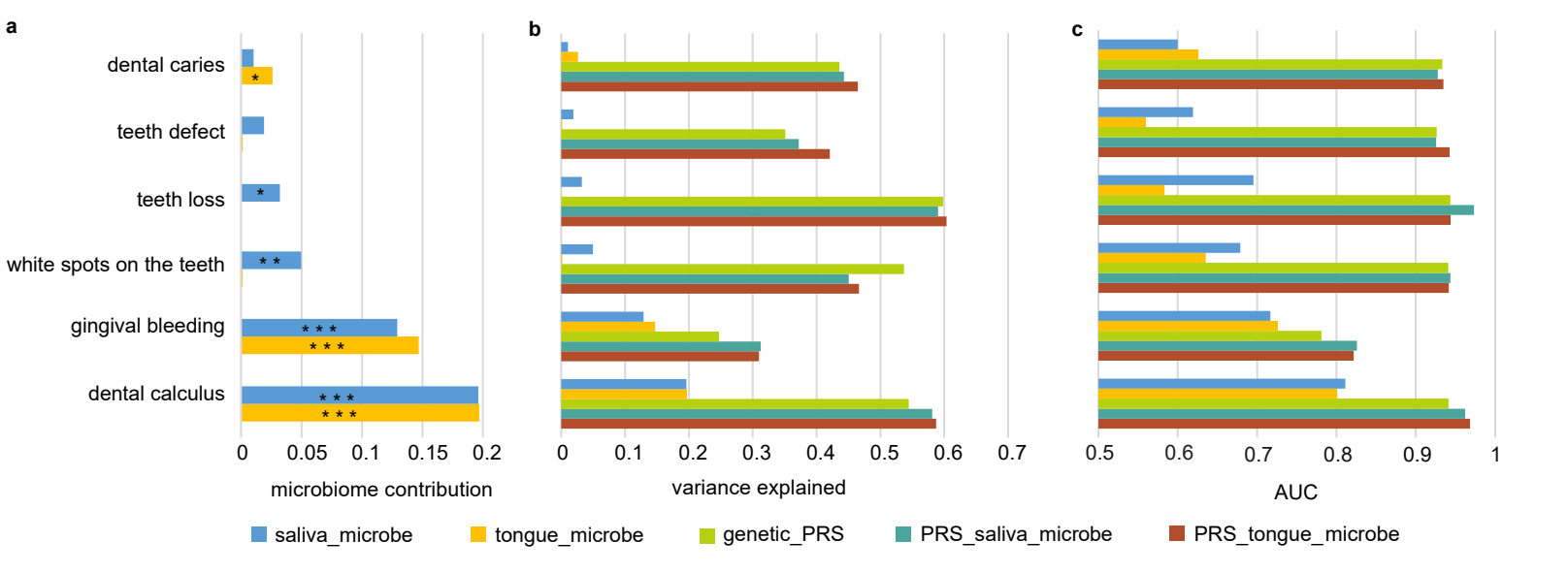
a
b
c
dental caries
teeth defect
teeth loss
white spots on the teeth
gingival bleeding
dental calculus
* * *
0
0.05
0.1
0.15
0.2
microbiome contribution
0.3
0.4
0.5
0.6
0.7
variance explained
0.6
0.7
0.8
0.9
1
AUC
saliva_microbe
tongue_microbe
genetic_PRS
PRS_saliva_microbe
PRS_tongue_microbe